

---

# Colorectal Cancer Imaging with Iodine-123-Labeled CEA Monoclonal Antibody Fragments

David M. Goldenberg, Theodore J. Wlodkowski, Robert M. Sharkey, Edward B. Silberstein, Aldo N. Serafini, Izak I. Garty, Ronald L. Van Heertum, Edith A. Higginbotham-Ford, Jon A. Kotler, N. Balasubramanian, Lawrence C. Swayne, Hans J. Hansen and Carl M. Pinsky

*Garden State Cancer Center at the Center for Molecular Medicine and Immunology, Newark, New Jersey; Immunomedics, Inc., Morris Plains, New Jersey; University of Cincinnati, Departments of Radiology and Medicine, Cincinnati, Ohio; University of Miami, Departments of Radiology and Medicine, Miami, Florida; St. Vincent's Hospital, Department of Radiology, New York, New York; University Hospital—New Jersey Medical School, Department of Nuclear Medicine, Newark, New Jersey; Department of Nuclear Medicine, Cleveland Clinic Florida, Ft. Lauderdale, Florida; Department of Nuclear Medicine, George Washington University, Washington, DC; and Department of Radiology, Morristown Memorial Hospital, Morristown, New Jersey*

---

This prospective, randomized multicenter study in 62 patients was designed to evaluate the efficacy and safety of radioimmunodetection (RAID) with <sup>123</sup>I-labeled fragments, F(ab')<sub>2</sub> and Fab', of IMMU-4, an anti-CEA monoclonal antibody (ImmuRAID-CEA). It was found that ImmuRAID-CEA was safe and disclosed colorectal cancer sites at least 1 cm in size. The positive predictive value by lesions was 77% initially, and increased to 91% after 7 mo of follow-up. Only one patient developed a low level of HAMA. In 17 patients with 32 surgically confirmed lesions, there were 9% true-positive lesions for CT when RAID was false-negative, and 22% for RAID when CT was false-negative. Either CT or RAID detected all 32 lesions. In this small series, therefore, RAID was shown to complement CT findings by confirming suspected tumors and disclosing new lesions which had previously been occult.

**J Nucl Med 1993; 34: 61-70**

---

**R**adiolabeled antibodies against a variety of tumor-related cellular constituents are gaining in acceptance as agents for the detection of cancer (1-6), including the disclosure of sites of malignancy which are missed by conventional procedures (7,8). This new approach has been called cancer radioimmunodetection (RAID) (9,10) and has involved several thousand patient studies with different antibodies, isotopes, and nuclear imaging procedures (1,11-15).

The first antigen that served as a target for RAID was carcinoembryonic antigen (CEA) (16). Antibodies to CEA labeled with <sup>131</sup>I have been the most widely used reagents

in RAID trials of diverse carcinomas, such as gastrointestinal, lung, breast, ovarian, and uterine cancers (17-20). These studies have involved the use of a variety of polyclonal and monoclonal antibodies (Mabs) and antibody fragments and different radionuclides, resulting in varying degrees of success in locating sites of cancer (20-30).

In two prior studies, Delaloye et al. (31,32) used <sup>123</sup>I-labeled CEA Mab fragments to image colorectal cancers and found that of known tumor sites 82% and 89% were detected by SPECT with 1-mg doses of F(ab')<sub>2</sub> and Fab Mab forms, respectively. The most accurate RAID images were obtained at 24 hr. Unfortunately, these investigators did not evaluate each tumor site individually, but combined them on an organ basis, resulting in an overall true-positive detection of 38 of 44 organs (86%) involved with tumor when the results with both antibody forms were combined. This method of data analysis can result in an overestimated detection rate in patients with advanced disease, where several tumor lesions per organ are present, particularly in liver with multiple metastases. In a second prospective study of <sup>123</sup>I-CEA Mab fragment imaging in 57 patients with CEA-producing tumors, using identical analysis criteria, the investigators reported an overall RAID sensitivity of 82%, which involved an 89%-93% sensitivity in patients with significant disease and a 71% sensitivity rate in patients with questionable colorectal cancer recurrence (32). A notable finding in this study was a sensitivity rate of liver metastases of 96%; however, this was accompanied by a false-positivity of 25% (32).

Since <sup>123</sup>I appeared to have distinct advantages over <sup>131</sup>I and <sup>111</sup>In for colorectal cancer imaging with CEA Mab fragments (for example, shorter half-life, more ideal energy for existing gamma cameras, less uptake in the liver than <sup>111</sup>In), we performed a multicenter, double-blind, prospective RAID trial comparing F(ab')<sub>2</sub> to Fab' at two Mab doses and at different imaging times and evaluated the results on a patient and tumor-lesion basis by planar and SPECT imaging procedures.

---

Received Mar. 20, 1992; revision accepted Aug. 17, 1992.  
For correspondence or reprints contact: David M. Goldenberg, MD, Center for Molecular Medicine and Immunology, 1 Bruce St., Newark, NJ 07103.

## MATERIALS AND METHODS

### Monoclonal Antibody

The anti-CEA Mab was IMMU-4 (NP-4) (33-35). IMMU-4 is a Class-III anti-CEA antibody (34) of the immunoglobulin IgG1 subclass with kappa light chains. It is specific for CEA, not reacting with antigens that share CEA-related epitopes, such as meconium antigen and normal cross-reactive antigens. It does not complex appreciably with circulating CEA below a titer of 500 ng/ml (36). To prepare Fab' and F(ab')<sub>2</sub>, ascites was produced in virus-free mice with the NP-4 hybridoma cell line. Then the ascites was aseptically removed, centrifuged to remove cells, and the supernatant was frozen and stored at -80° C. After thawing, the supernatant was further clarified by passing through an ion-exchange column using pH and ionic conditions that prevented binding of the IMMU-4 to the ion-exchange matrix. IgG was isolated from the clarified supernatant by Protein A affinity chromatography and further purified by ion-exchange chromatography. Purity and identity were proven by immunoelectrophoresis, SDS gel electrophoresis, and isoelectric focusing. IgG was converted to F(ab')<sub>2</sub> by pepsin digestion and purified by gel filtration chromatography and ion-exchange chromatography. Purified F(ab')<sub>2</sub> was reduced to Fab' with cysteine. The cysteine was removed by gel filtration and the Fab'-SH was alkylated with iodoacetamide. Excess iodoacetamide was removed by gel filtration chromatography.

The IMMU-4 monoclonal antibody was supplied in a double-blind manner as a coded, sterile, nonpyrogenic solution in two vials. The first vial contained 1 mg of the appropriate F(ab')<sub>2</sub> or Fab' fragment to be radiolabeled. The second vial contained an additional 9 mg of the appropriate "cold" antibody fragment or human serum albumin. The contents of the second vial were mixed with the radiolabeled material prior to administration to the patient. The antibody preparations were shown to be safe for clinical use by microbiological, acute toxicity, and pyrogenicity testing.

### Radioiodination

The antibody fragments were radiolabeled using chloramine-T (37) at the investigator's facility with <sup>123</sup>I obtained from Nordion International, Inc. (Kanata, Ontario, Canada). The final product containing 8-10 mCi of <sup>123</sup>I was filtered through a 0.22- $\mu$ m Millipore filter (Millipore, Bedford, MA). Iodine incorporation was determined by comparing free and protein-bound iodine on silica gel thin-layer radiochromatography (ITLC) in an acetone buffer system. Immunoreactivity of the radiolabeled fragments was determined by affinity chromatography on a CEA immunosorbent (38).

### Patient Selection

Ambulatory male and female patients with cancer of the colon or rectum were included if they were 21 yr of age or older and: (a) had at least one known lesion at least 1 cm in size; (b) had a histologically confirmed diagnosis of colorectal cancer; (c) were off chemotherapy, other experimental anti-cancer therapy, or radiotherapy for 1 wk before or after Mab infusion; (d) had Karnofsky status of at least 60%; (e) had no prior exposure to mouse antibodies or known allergies to mouse proteins; and (f) were not women who were pregnant or who were lactating. All patients were skin-tested for hypersensitivity to IMMU-4 (5  $\mu$ g in 0.02 ml injected intradermally and read at 15 min). The protocol was approved by the institutional review board at each partici-

pating institution, and informed consent was obtained from each subject after the nature of the procedures and potential risks were explained.

### Study Design

This was a prospective, randomized, double-blind, parallel-group multicenter trial. To minimize thyroid sequestration of <sup>123</sup>I, patients were placed on Lugol's iodine (KI) starting three days before the Mab administration (0.9 g three times daily). To inhibit secretion of the radioiodine in the intestinal tract, patients were given potassium perchlorate immediately before antibody infusion (200 mg). Patients received either two doses (1 mg or 10 mg) of either of the two fragments, F(ab')<sub>2</sub> or Fab', of IMMU-4. Iodine-123-labeled (8-10 mCi) anti-CEA antibody fragment diluted with 30 ml of sterile saline was infused intravenously via a buretrol over a 20 to 30-min period. The patients continued to receive Lugol's iodine and potassium perchlorate for two days postinfusion. Planar or tomographic imaging, or both, was performed at 2 to 4 hr, 24 hr, and 48 hr after antibody injection.

### Imaging Technique

Several different gamma cameras and computer systems were used in this trial, but one general protocol was followed. Planar images were obtained at 2 to 4, 24, and 48 hr postinfusion over the head, chest, abdomen, and pelvis in anterior, posterior, and lateral projections. Counts in the range of 250,000 to 500,000 were acquired per view, except at the 48-hr imaging time, when 100,000 to 300,000 counts were acquired per view. A high-resolution, low-energy, parallel-hole collimator was usually used or, if not available, a low-energy, all-purpose collimator was employed. Single-photon emission computed tomography (SPECT) was performed at 4 and/or 24 hr postinfusion, acquiring three regions, chest, abdomen, and pelvis, in transaxial, coronal, and sagittal slices of 3.3 mm thickness. The 360° orbit consisted of 128 projections at an acquisition of 12 to 15 sec/angle in a 128  $\times$  128 format. In some centers a 64  $\times$  64 matrix was used.

### Efficacy Evaluation

All patients received an examination of the liver by CT, usually just before or after the radionuclide antibody study, employing current instrumentation. Initially, the CT and RAID scans were read independently of each other, with full knowledge of the clinical history. CT scans and RAID scans were then compared (side-by-side) and scored. One of us (L.C.S.) correlated the CT and antibody scans (without knowledge of the clinical history) in those cases where the initial interpretations from the study sites were not perfectly clear. Separate analyses were performed on images obtained at 2 to 4 hr, 24 hr, and 48 hr postinfusion. Sensitivity was calculated on a lesion-site basis using the following formula: TP/(TP + FN). Specificity on a region basis was calculated as: TP/(TN + FP). Accuracy also determined on a regional basis was calculated as: (TP + TN)/(TP + TN + FP + FN). Positive predictive value was calculated on a lesion-site basis using the following formula: TP/(TP + FP). Negative predictive value on a region basis was calculated as: TN/(TN + FN). At 5 min, 1 hr, 2 to 4 hr, 24 hr and 48 hr postinfusion, blood samples were analyzed for pharmacokinetics. In one case, a patient who was scheduled for surgery within 48 hr of the infusion provided samples of tumor and adjacent normal tissue for isotope counting purposes and histopathology evaluation.

## Safety Evaluation

A medical history and physical examination were performed at baseline. A panel of studies consisted of: complete blood count with differential and platelet counts; blood chemistry evaluations, including total protein, calcium, phosphorus, blood sugar, BUN, creatinine, total bilirubin, uric acid, alkaline phosphatase, LDH, SGOT, and SGPT. A urinalysis was performed at baseline and at specified timepoints throughout the study to detect any toxic effects of the infusion. Blood samples obtained before and after antibody administration were also tested for CEA level and the development of HAMA. HAMA was quantitated using the commercial research ImmuSTRIP® HAMA Kit (Immunomedics, Inc., Morris Plains, NJ) (39,40). Samples for detection of HAMA development were obtained prior to infusion and at 2 to 4 wk following the infusion.

## RESULTS

### Study Population

Sixty-two patients (40 males and 22 females, 29 to 81 yr old) with colorectal cancer were enrolled by the six centers. Two patients did not receive the complete antibody IMMU-4 fragment dose. One patient was entered into the study with only a rising CEA level and no proven tumor sites. One patient received the Mab infusion but was not scanned. These four patients were excluded from efficacy analysis but were evaluated for safety. The demographic characteristics of the patient population are given in Table 1 for those patients who were evaluable for

efficacy. There were no significant differences between the four study groups; all groups were comparable with regard to age, sex, stage at infusion, and duration of disease.

### Efficacy

Of the 58 patients evaluable for efficacy, 17 received 1 mg of F(ab')<sub>2</sub>, 14 received 10 mg of F(ab')<sub>2</sub>, 12 received 1 mg of Fab', and 15 received 10 mg of Fab'. For the entire group of studies, ITLC revealed an average of 87% incorporation of <sup>125</sup>I. Immunoreactivity after radioiodination varied from 73% to 80%, with no statistically significant differences between the four arms of the study when analysis of variance (ANOVA) was used.

The results summarized in Table 2 indicate that of the three time frames tested, the 24-hr interpretation gave the highest lesion sensitivity for previously known colorectal cancer lesions. The localization of tumor versus background at 2 hr was insufficient for useful imaging, while at 48 hr the absolute number of counts was insufficient for good image interpretation.

Perhaps the most important parameter in this study was the lesion-by-lesion positive predictive value, which was 77% overall when calculated on the basis of available data at the time of RAID. After 7 mo of follow-up, when additional clinical findings became available, the positive predictive value increased to 91%. The overall imaging results, with 95% confidence intervals expressed in terms of sensitivity, specificity, and accuracy, are shown in Figure

**TABLE 1**  
Frequency Table Analysis of Demographic Data

| Variable                   | Group                       |                              |              |                  | $\chi^2$ | d.f. | p-value |
|----------------------------|-----------------------------|------------------------------|--------------|------------------|----------|------|---------|
|                            | F(ab') <sub>2</sub><br>1 mg | F(ab') <sub>2</sub><br>10 mg | Fab'<br>1 mg | Fab'<br>10 mg    |          |      |         |
| Sex                        |                             |                              |              |                  |          |      |         |
| Male                       | 14                          | 11                           | 7            | 7                | —        | —    | —       |
| Female                     | 3                           | 3                            | 5            | 8                | 6.10     | 3    | >0.10   |
| Age (yr)                   |                             |                              |              |                  |          |      |         |
| ≤50                        | 2                           | 3                            | 1            | 1                | —        | —    | —       |
| 51–60                      | 4                           | 3                            | 4            | 3                | —        | —    | —       |
| 61–70                      | 9                           | 5                            | 4            | 6                | —        | —    | —       |
| >70                        | 2                           | 3                            | 3            | 5                | 4.59     | 9    | >0.80   |
| Stage at infusion          |                             |                              |              |                  |          |      |         |
| Dukes B                    | 1                           | 1                            | 3            | 1                | —        | —    | —       |
| Dukes C                    | 0                           | 0                            | 1            | 0                | —        | —    | —       |
| Dukes D                    | 14                          | 12                           | 8            | 13               | —        | —    | —       |
| (Not Recorded)             | (2)                         | (1)                          | (0)          | (1)              | 6.98     | 6    | >0.30   |
| Weight (lb)                |                             |                              |              |                  |          |      |         |
| ≤125                       | 2                           | 1                            | 1            | 0                | —        | —    | —       |
| 126–175                    | 12                          | 9                            | 7            | 10               | —        | —    | —       |
| 176–225                    | 2                           | 3                            | 2            | 3                | —        | —    | —       |
| >225                       | 0                           | 1                            | 1            | 1                | 4.01     | 9    | >0.90   |
| Duration of disease (days) |                             |                              |              |                  |          |      |         |
| ≤1000                      | 14                          | 9                            | 10           | 6                | —        | —    | —       |
| 1001–2000                  | 3                           | 2                            | 1            | 8                | —        | —    | —       |
| 2001–3000                  | 0                           | 2                            | 1            | 1                | —        | —    | —       |
| >3000                      | 0                           | 1                            | 0            | 0                | 16.4     | 9    | >0.05   |
|                            |                             |                              |              | $\Sigma\chi^2 =$ | 38.08    | 36   | >0.30   |

**TABLE 2**  
Detection of Known Lesions with <sup>125</sup>I Label

|           | F(ab') <sub>2</sub> 1 mg |                   |                   | F(ab') <sub>2</sub> 10 mg |                   |                   |
|-----------|--------------------------|-------------------|-------------------|---------------------------|-------------------|-------------------|
|           | 2 hr<br>(n = 34)         | 24 hr<br>(n = 38) | 48 hr<br>(n = 35) | 2 hr<br>(n = 38)          | 24 hr<br>(n = 38) | 48 hr<br>(n = 29) |
| Positive  | 41%                      | 79%               | 60%               | 34%                       | 71%               | 38%               |
| Negative  | 56%                      | 16%               | 29%               | 66%                       | 29%               | 62%               |
| Equivocal | 3%                       | 8%                | 11%               | 0%                        | 0%                | 0%                |

|           | Fab' 1 mg        |                   |                   | Fab' 10 mg       |                   |                   |
|-----------|------------------|-------------------|-------------------|------------------|-------------------|-------------------|
|           | 2 hr<br>(n = 34) | 24 hr<br>(n = 35) | 48 hr<br>(n = 34) | 2 hr<br>(n = 33) | 24 hr<br>(n = 37) | 48 hr<br>(n = 34) |
| Positive  | 44%              | 83%               | 62%               | 61%              | 86%               | 71%               |
| Negative  | 56%              | 14%               | 38%               | 24%              | 11%               | 26%               |
| Equivocal | 0%               | 3%                | 0%                | 15%              | 3%                | 3%                |

1 for the 24-hr images. In addition, of particular note were the imaging findings in the liver (not shown), where sensitivity was 89%, specificity was 80% and accuracy was 86%.

Sensitivity, specificity, and accuracy for all regions and all four arms of the study initially were 77%, 81%, and 79%, respectively. After almost 7 mo of follow-up, the sensitivity, specificity, and accuracy increased to 86%, 89% and 89%, respectively. Although 12 to 17 patients were analyzed per antibody fragment/dose group, the results involved a total of 62 to 78 body sites per group. We did not observe any differences between the imaging results of the four groups (*p* = ns). There does not appear to be a dose dependence for the targeting of the radiolabeled antibody fragments to the tumors, although there does appear to be a statistically insignificant advantage to the Fab' fragment sensitivity. The results appear to indicate that 1 mg of Fab' was sufficient to image known lesions. There appeared to be no correlation between sensitivity and size of lesions or serum CEA level. SPECT evaluation was

judged to be more beneficial than planar imaging in 27 of 58 patients (47%), because of such factors as avoidance of misinterpretation of urethral artifact and scatter from the bladder and better definition of the number and size of liver lesions.

A comparison of CT versus RAID results in 17 patients with 33 apparent lesions who underwent surgery after the RAID study indicated that 22 of the 32 surgically-confirmed lesions were positive both by CT and RAID, whereas 100% of the surgically confirmed lesions were positive by either CT or RAID. One patient, who had surgery performed two days after infusion of the radiolabeled antibody fragment, had scintillation counting of biopsied specimens. In this patient with liver metastasis, the tumor-to-liver ratio was 19-to-1. Three surgically confirmed tumor lesions were positive by CT and negative by RAID. Seven of eight lesions that were positive by RAID and negative by CT scan were confirmed as cancer at surgery. The eighth lesion was reported as a hepatic cyst at surgery. However, the nuclear medicine investigator (A.N.S.) did not believe that the 10-mm cyst observed during surgery corresponded to the localization seen on RAID scan. While, the surgeon did not biopsy the suspected area of the liver, with no positive CT findings within the year following the RAID scan, this localization was categorized as a false-positive. This series indicated that CT was positive in 78% of the surgically confirmed lesions and RAID was positive in 91%; RAID missed only 9% of lesions disclosed by CT, while CT missed 22% of the tumors revealed by RAID. Both methods were positive in 22 of 32 (69%) cases, all of which proved to be cancer on biopsy. This indicates that when RAID-positive lesions are confirmed at the same anatomical location by another noninvasive imaging method one can reliably conclude that cancer is present, even without histological confirmation. Three illustrative cases in which RAID detected

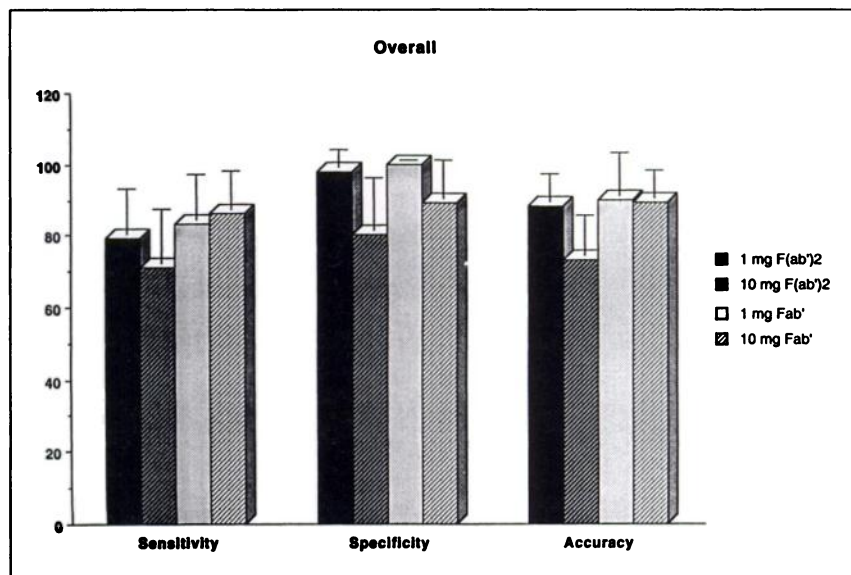


**FIGURE 1.** Overall sensitivity, specificity, and accuracy for each of the labeled antibody fragments. Error bars represent the upper 95% confidence interval.

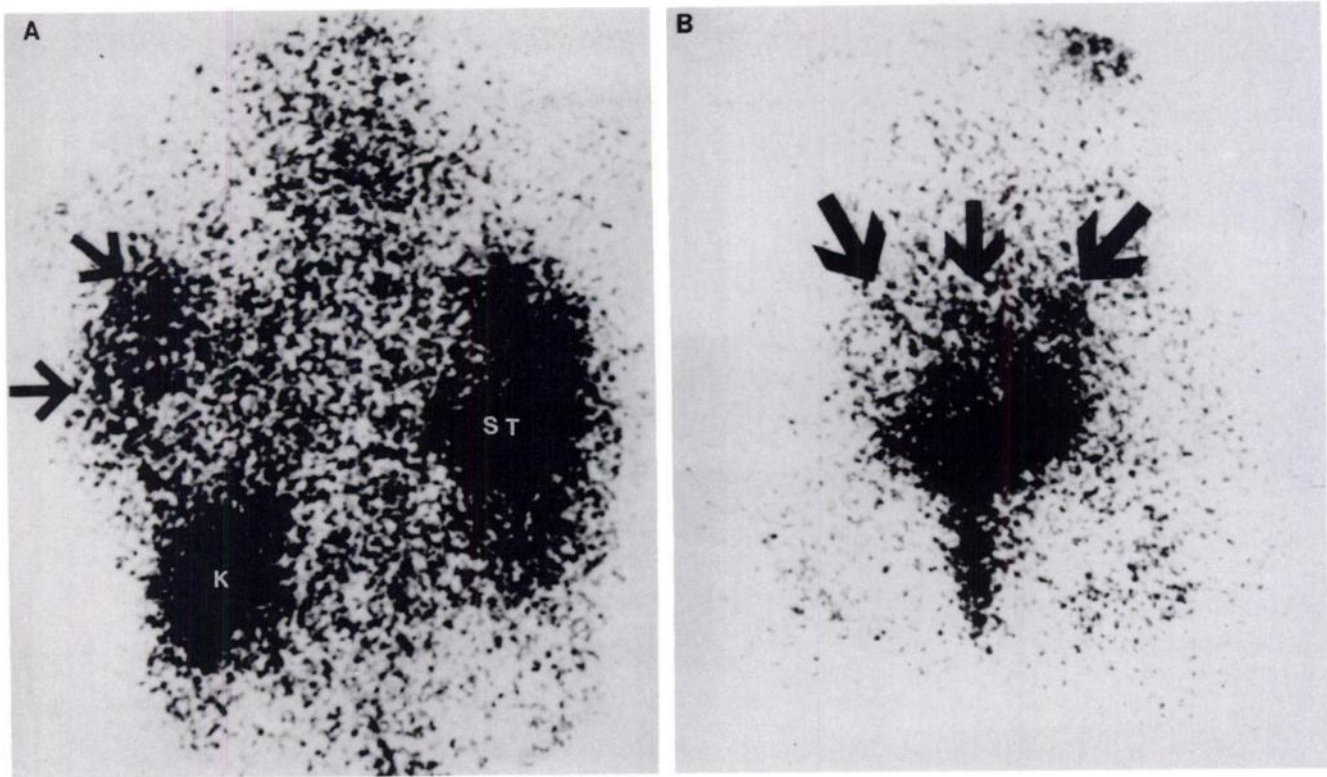


**FIGURE 2.** A 53-yr-old female with carcinoma of the sigmoid colon and known metastatic spread to the liver. (A) Anterior planar view from radioimmunoscintigraphy performed 24 hr after the administration of IMMU-4 antibody fragments. Arrows point to pathological uptake in areas which correspond to known metastatic liver lesions. Also note physiological uptake in kidney (K) and stomach (ST). (B) Posterior planar view. Previously undetected diffuse concentration above the urinary bladder (arrows) more clearly seen in the right side, which was compatible with local recurrence of the disease with lymph node metastatic spread near the primary tumor site. These previously occult lesions were confirmed by subsequent CT scan and exploratory laparotomy.

previously occult lesions are presented in Figures 2–4. Overall, on a patient-by-patient basis, the sensitivity was 88% and the positive predictive value was 96%.

A total of 30 new lesions were detected, which were not disclosed by other detection methods (Table 3). The number of new lesions found by RAID are indicated in the found column (30); the number of lesions that had appropriate follow-up are given in the followed column (25); and the number of lesions confirmed as cancer are pro-

vided in the confirmed column (18). Seventy-two percent of these new lesions have been confirmed by CT, x-ray, or surgery/biopsy within an almost 7-mo follow-up period. This directly led to clinical benefit in 13 (22%) patients due to more appropriate therapy or instituting additional diagnostic studies.

A pharmacokinetic study performed at the Center for Molecular Medicine and Immunology, which determined radioantibody half-life in blood by curve-fitting five data

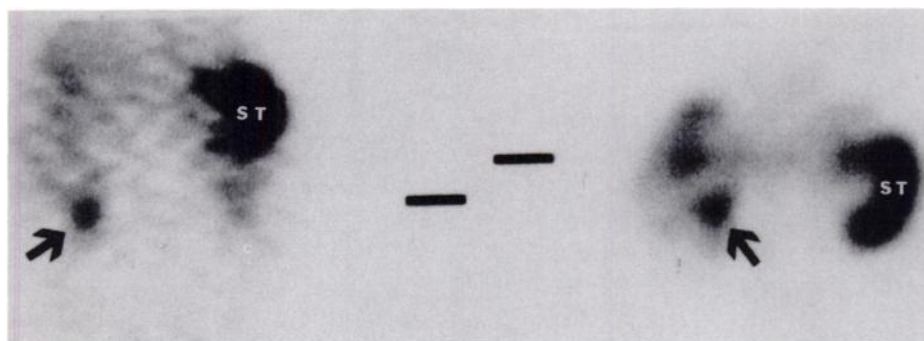


**FIGURE 3.** A 50-yr-old male with carcinoma of the transverse colon and known progressive metastatic disease to the liver. In addition to confirming the known liver lesions (not shown), a SPECT study of the abdomen shows previously occult focal uptake below the liver (arrow). (Coronal section left. Sagittal section right.) Metastatic lymphatic spread to the celiac axis was verified by a subsequent follow-up CT scan and explorative laparotomy. Note physiological activity of  $^{123}\text{I}$  in the stomach (ST).

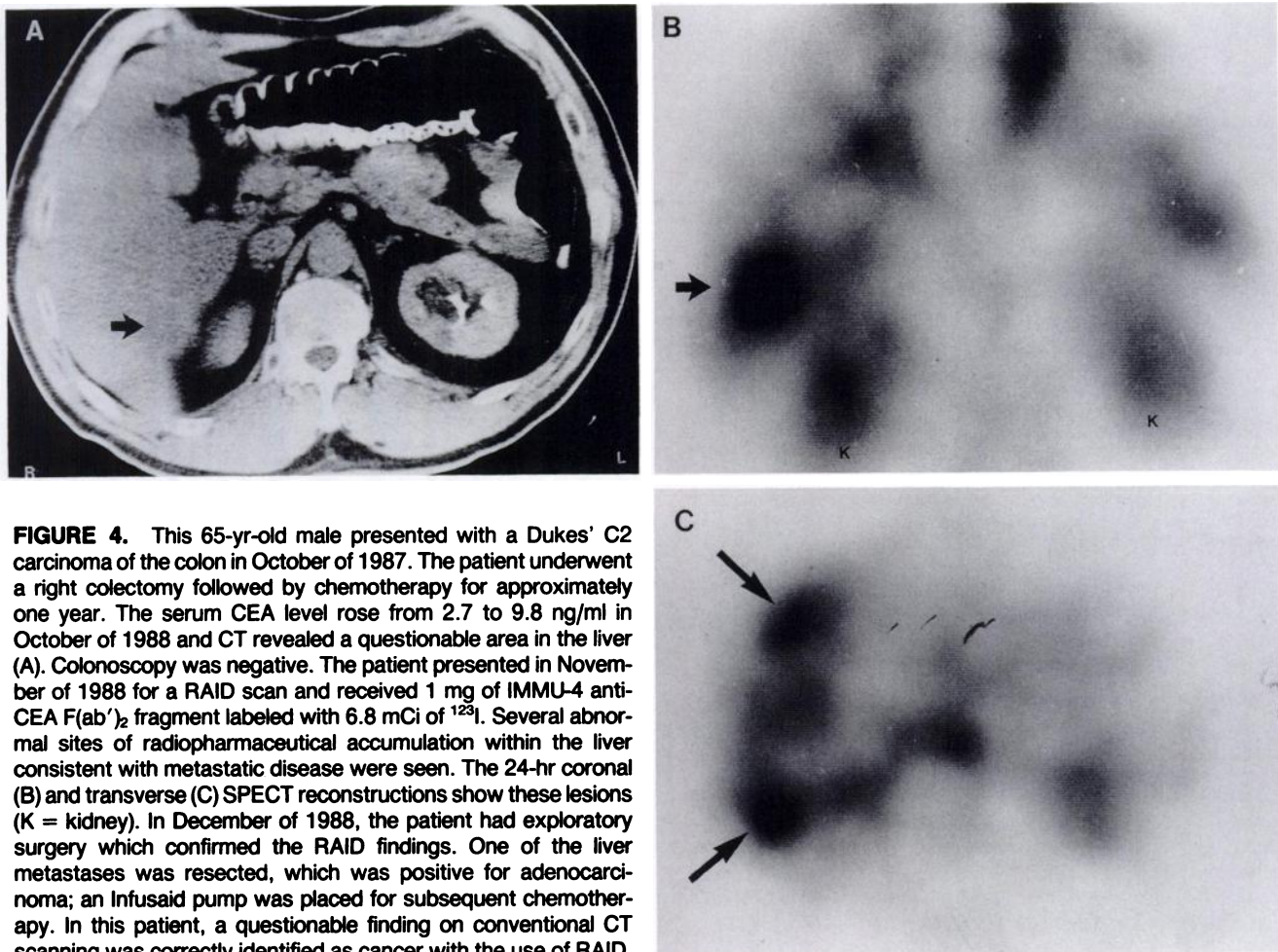


**FIGURE 4.** This 65-yr-old male presented with a Dukes' C2 carcinoma of the colon in October of 1987. The patient underwent a right colectomy followed by chemotherapy for approximately one year. The serum CEA level rose from 2.7 to 9.8 ng/ml in October of 1988 and CT revealed a questionable area in the liver (A). Colonoscopy was negative. The patient presented in November of 1988 for a RAID scan and received 1 mg of IMM-4 anti-CEA F(ab')<sub>2</sub> fragment labeled with 6.8 mCi of <sup>123</sup>I. Several abnormal sites of radiopharmaceutical accumulation within the liver consistent with metastatic disease were seen. The 24-hr coronal (B) and transverse (C) SPECT reconstructions show these lesions (K = kidney). In December of 1988, the patient had exploratory surgery which confirmed the RAID findings. One of the liver metastases was resected, which was positive for adenocarcinoma; an Infusaid pump was placed for subsequent chemotherapy. In this patient, a questionable finding on conventional CT scanning was correctly identified as cancer with the use of RAID.

points, yielded the results presented in Figure 5. The median biological half-lives of the F(ab')<sub>2</sub> and Fab' in the blood, measured during the distribution ( $\alpha$ ) phase, were 1.6 and 2.4 hr, respectively. The median biological half-lives of the F(ab')<sub>2</sub> and Fab' in the blood, measured during the elimination ( $\beta$ ) phase, were 26 and 19 hr, respectively.

Utilizing the 1-hr blood pharmacokinetics specimens from the nine University Hospital (UMDNJ) patients, we examined whether complexation of the antibody fragments with circulating CEA, HAMA, etc., could interfere with image quality. Two patients showed elevated 1-hr plasma complexation. One patient who received 1 mg of F(ab')<sub>2</sub> had 82% complexation and one patient who received 1 mg of Fab' had 13.6% complexation. Both patients also had elevated serum CEA levels (>10,000 ng/ml and 613 ng/ml, respectively). This degree of plasma complexation did not appear to interfere with the ability to image tumors. In the remaining patients, complexation ranged from 3.5% to 6.4%.

#### Safety

All of the 62 patients who received the anti-CEA monoclonal antibody IMM-4 fragments were evaluated for

adverse reactions. No significant changes were noted in the laboratory studies of blood or urine obtained 24 hr postinfusion. One patient reported a facial rash the evening of the infusion which disappeared by the next morning, so it was not observed by the principal investigator or staff. All laboratory abnormalities observed were consistent with the patients' underlying disease and did not worsen after antibody administration. Testing for HAMA was carried out in most of the patients. Fifty-two patients had adequate pre- and postinfusion serum samples for HAMA analysis. Two patients (4%) were found to have detectable HAMA prior to the infusion. One of these two patients was also positive for rheumatoid factor. Follow-up samples on these two patients revealed no increased titer after infusion. One patient (2%) treated with 10 mg of IMM-4 F(ab')<sub>2</sub>, who did not have pre-existing HAMA, developed a low level of antibody (159 ng/ml) during the course of study. Forty-nine patients (94%) showed no HAMA development.

#### DISCUSSION

This multicenter study of 62 patients demonstrates that IMM-4 anti-CEA Fab' and F(ab')<sub>2</sub> fragments labeled

**TABLE 3**  
New Lesion Sites (Efficacy Patients Only)

|                           | Found | Followed | Confirmed | Method of confirmation | Time to confirmation |
|---------------------------|-------|----------|-----------|------------------------|----------------------|
| 1 mg F(ab') <sub>2</sub>  | 8     | 7        | 6         | CT                     | At time of RAID scan |
|                           |       |          |           | CT                     | At time of RAID scan |
|                           |       |          |           | CT                     | At time of RAID scan |
|                           |       |          |           | Surgery                | 1 mo                 |
|                           |       |          |           | Surgery                | 1 mo                 |
| 10 mg F(ab') <sub>2</sub> | 8     | 6        | 3         | CT                     | 3.5 mo               |
|                           |       |          |           | L/S scan               | At time of RAID scan |
|                           |       |          |           | CT                     | 2 mo                 |
| 1 mg Fab'                 | 4     | 4        | 3         | CT                     | 3.33 mo              |
|                           |       |          |           | X-ray                  | At time of RAID scan |
| 10 mg Fab'                | 10    | 8        | 6         | Surgery                | 5 days               |
|                           |       |          |           | Biopsy                 | 1.5 mo               |
|                           |       |          |           | CT                     | At time of RAID scan |
|                           |       |          |           | CT                     | 2 wk                 |
|                           |       |          |           | Surgery                | 3 wk                 |
|                           |       |          |           | Surgery                | 3 wk                 |
| Total                     | 30    | 25       | 18 (72%)  | X-ray                  | 6 mo                 |
|                           |       |          |           | Surgery                | 6.75 mo              |

with <sup>123</sup>I can be given safely to patients with suspected recurrence or metastasis of colorectal cancer. Colorectal cancer sites at least 1 cm in size at many body sites can be confirmed and new lesions can be uncovered frequently before they are detectable by other diagnostic modalities. Fab' fragment doses as low as 1 mg are sufficient to obtain these results. Of the times tested, the optimal scanning time is 24 hr. Confirmation that new tumor sites detected are cancer can take up to 7 mo or longer.

Overall, these findings suggest that combined RAID with the IMMU-4 Fab' fragment and CT examination provides greater accuracy in the detection and localization of recurrent or metastatic colorectal cancer sites than CT alone (100% versus 78%). These results suggest that RAID (which is a functional test) and CT (which is limited to structural information) are complementary; that is, each finds different lesions. In contrast to other imaging techniques, antibodies labeled with the appropriate radioisotope have the potential to detect foci of cancer cells at multiple sites in the body with a single injection and imaging session, thus possibly being cost-effective. The procedure can also be helpful in directing other diagnostic procedures, such as CT and MRI, to specific areas. This can have clinical significance, since patient management decisions may be affected.

The use of radiolabeled antibodies to image patients with cancer has been in progress for nearly 15 yr (1,2,20, 41-46). Despite such a large experience, no product has been adopted in the U.S. for general use. An acceptable agent must be safe, easy to use, yield clear-cut images on available nuclear medicine equipment, and provide clinically relevant information to the practitioner. We believe that this report provides preliminary data which satisfy these requirements. Clearly, the product appears to be safe,

causing virtually no side effects and inducing a low level of HAMA in only one patient. The data reported here, supplemented by observations on 38 additional patients imaged at The Center for Molecular Medicine and Immunology (23), indicate a high level of safety. Furthermore, the agent has proven to be relatively easy to use with readily adopted iodine-labeling techniques. Quality control has been excellent in the field, with 87% incorporation of the <sup>123</sup>I into the conjugate and immunoreactivity of the conjugate averaging 76% using a CEA-affinity column (38).

The quality and reliability of the images have been quite good, with the following initial imaging statistics: a positive predictive value of 77%; a negative predictive value of 84%; sensitivity of 77%; specificity of 81%; and accuracy of 79%. After follow-up, the statistics improve to: a positive predictive value of 91%; a negative predictive value of 84%; sensitivity of 86%; specificity of 89%; and accuracy of 89%. These results did not appear to be influenced by tumor size or serum CEA titer, which is in disagreement with some previous studies [reviewed in Goldenberg et al. (1)].

It is difficult to compare these clinical results with those reported in the literature, because each investigator analyzes the statistics differently (e.g., some by patient, some by region or organ, and some on a lesion-by-lesion basis). On an organ-site basis, Delaloye et al. (31,32) used <sup>123</sup>I-labeled anti-CEA fragments and observed 82% and 86% detection rates (sensitivity), respectively, in two studies. In their second study (32), earlier diagnosis on RAID scanning compared to conventional techniques was evident in 10 of 21 lesions.

F(ab')<sub>2</sub> fragments of an anti-CEA antibody labeled with either <sup>131</sup>I or <sup>111</sup>In were studied in a multicenter trial

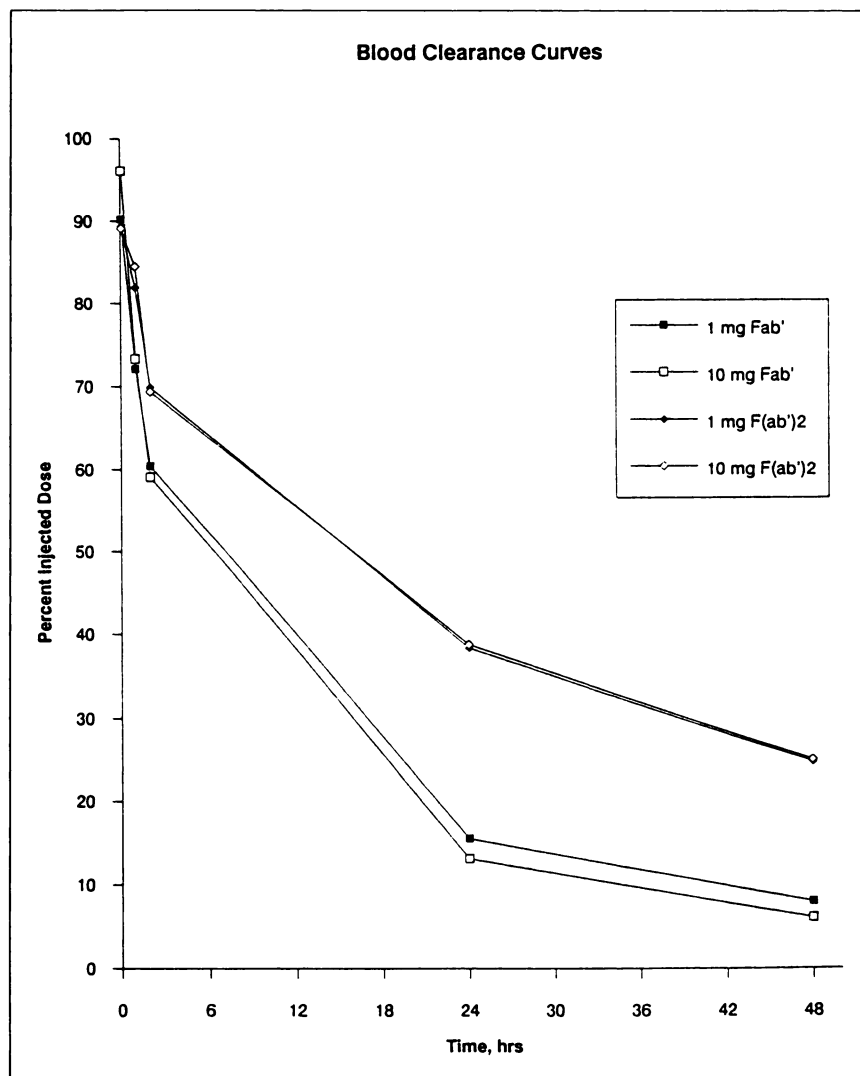


**FIGURE 5.** Blood clearance of the radiolabeled antibody fragments clearly demonstrates the more rapid clearance of the Fab' fragment. Note that at 24 hr only 10%–20% of the injected dose of the Fab' fragment remains in the blood, whereas approximately 40% of the F(ab')<sub>2</sub> fragment remains.

involving 488 patients with various CEA-producing tumors (284 from the gastrointestinal tract) (22). Detection of known lesions was 73% for patients with elevated serum CEA and only 54% when the CEA level was normal. In 35 patients, detection of previously occult lesions led to earlier diagnosis of recurrence or metastasis.

In comparing this study with those in the literature, one other factor is important. In the trial reported here, only one patient developed a low level of HAMA, compared to 40%, 23%, or 31%, respectively, in three previously reported studies employing intact murine immunoglobulin (47,48). Presumably this difference is due to the use of fragment rather than intact antibody, but one cannot rule out the possibility that IMM-4 is a low immunogenic antibody.

Clinical benefit can be defined in a number of ways, but primarily derives from detecting tumors missed by conventional noninvasive techniques. Initially, lesions seen only on RAID scans should be classified as false-positive, until follow-up demonstrates that they were correctly di-

agnosed as cancers. In this study, 18 of 25 such lesions could be shown to be malignant tumors within almost 7 mo, resulting in clinical benefit to 13 of the patients. Furthermore, surgical exploration in 17 patients demonstrated that antibody imaging disclosed more cancerous lesions (29) than CT scans (25). Had RAID scans not been performed, seven lesions in seven patients might not have been resected. Thus, the total number of patients who had clinical benefit was 22% of the 58 evaluable patients.

The data also showed that three surgically confirmed tumor lesions were positive by CT and negative by RAID. All three lesions were large primary tumors (two sigmoidal and one rectal) in three different patients. SPECT imaging was not available in two of the three cases, and all three patients were among the earliest patients entered at their respective institutions. Histopathology on the surgical specimens indicated tumor necrosis and focal necrosis with calcification. Considerations that may explain the negative RAID findings include poor tumor blood flow, vascular

permeability, reduced tumor metabolism, increased interstitial pressure, and a lack of lymphatic pathways in the tumors (17,49,50).

In addition to such clinical end-points, this study was designed to determine, in a blinded fashion, whether there was a preference for the Fab' or the F(ab')<sub>2</sub> fragment at doses of 1 mg and 10 mg. It was shown that 1 mg of the Fab' fragment confirmed as many known lesions as did 10 mg of Fab', or either dose of F(ab')<sub>2</sub>. In subsequent studies, we have concentrated on agents using 1 mg of the Fab' fragment labeled by a simple, direct method with <sup>99m</sup>Tc (23,27,51).

## ACKNOWLEDGMENTS

This study was supported by Immunomedics, Inc. and in part by USPHS grant CA39841 from the NIH (D.M.G.). We thank Ms. Tori Mutz, Mr. Ted Palm, Mr. Robert Cuddihy, Mr. Thomas Feld and Mr. Robert E. Lee for their expert help in preparing the manuscript.

## REFERENCES

1. Goldenberg DM, Goldenberg H, Sharkey RM, et al. Imaging of colorectal carcinoma with radiolabeled antibodies. *Semin Nucl Med* 1989;19:262-281.
2. Goldenberg DM, ed. *Cancer imaging with radiolabeled antibodies*. Norwell, MA: Kluwer Academic Publishers, 1990:1-417.
3. Merchant B. Monoclonal antibody-based imaging of colorectal carcinoma. Presented at "Current status and future directions in immunoconjugates—diagnostic and therapeutic applications", Orlando, FL, October 15-17, 1990.
4. Lamki LM, Patt YZ, and Murray JL. In-111 monoclonal antibody immunoscintigraphy of colorectal cancer. In: Goldenberg DM, ed. *Cancer imaging with radiolabeled antibodies*. Norwell, MA: Kluwer Academic Publishers; 1990:293-312.
5. Eary JF, Schroff RW, Abrams PG, et al. Successful imaging of malignant melanoma with technetium-99m-labeled monoclonal antibodies. *J Nucl Med* 1989;30:25-32.
6. Beatty JD, Hyams DM, Morton BA, et al. Impact of radiolabeled antibody imaging on management of colon cancer. *Am J Surg* 1989;157:13-19.
7. DeLand FH, Kim EE, Casper S, et al. Radioimmunodetection of occult recurrent colonic carcinoma. *AJR* 1982;138:145-148.
8. Goldenberg DM, Kim EE, Bennett SJ, Nelson MO, DeLand F. Carcinoembryonic antigen radioimmunodetection in the evaluation of colorectal cancer and in the detection of occult neoplasms. *Gastroenterology* 1983;84:524-532.
9. Goldenberg DM. Immunodiagnosis and immunodetection of colorectal cancer. *Cancer Bull* 1978;30:213-218.
10. Goldenberg DM, Primus FJ, Kim E, et al. Radioimmunodetection of cancer. In: Boelsma E, Rumke PH, eds. *Tumour markers: impact and prospects*. Amsterdam: Elsevier/North Holland Biomedical Press; 1979:167-177.
11. Bradwell AR, Fairweather DS, Dykes PW, et al. Limiting factors in the localization of tumors with radiolabeled antibodies. *Immunol Today* 1985;6:163-170.
12. Chatal JF, Saccavini JC, Fumoleau P, et al. Immunoscintigraphy of colon carcinoma. *J Nucl Med* 1984;25:307-314.
13. Carrasquillo JA, Sugarbaker P, Colcher D, et al. Radioimmunoscintigraphy of colon cancer with iodine-131-labeled B7.2 monoclonal antibody. *J Nucl Med* 1988;29:1022-1030.
14. Nelson MO, DeLand FH, Shochat D, et al. External imaging of gastric cancer metastases with radiolabeled CEA and CSAP antibodies [Letter]. *N Engl J Med* 1983;308:847.
15. Armitage NC, Perkins AC, Pimm MV, et al. The localization of an anti-tumor monoclonal antibody (791T/36) in gastrointestinal tumors. *Br J Surg* 1984;71:407-412.
16. Primus FJ, Wang RH, Goldenberg DM, Hansen HJ. Localization of human GW-39 tumors in hamsters by radiolabeled heterospecific antibody to carcinoembryonic antigen. *Cancer Res* 1973;33:2977-2982.
17. Goldenberg DM, DeLand F, Kim E, et al. Use of radiolabeled antibodies to carcinoembryonic antigen for detection and localization of diverse cancers by external photoscanning. *N Engl J Med* 1978;298:1384-1388.
18. Goldenberg DM, Kim EE, DeLand FH, et al. Radioimmunodetection of cancer with radioactive antibodies to carcinoembryonic antigen. *Cancer Res* 1980;40:2984-2992.
19. Van Nagell JR Jr, Kim E, Casper S, et al. Radioimmunodetection of primary and metastatic ovarian cancer using radiolabeled antibodies to carcinoembryonic antigen. *Cancer Res* 1980;40:502-506.
20. Goldenberg DM, Larson SM. Radioimmunodetection in cancer identification. *J Nucl Med* 1992;33:803-814.
21. Carrasquillo JA, Krohn KA, Beaumier P, et al. Diagnosis and therapy for solid tumors with radiolabeled antibodies and immune fragments. *Cancer Treat Rep* 1984;68:317-328.
22. Siccardi AG, Buraggi GL, Callegaro L, et al. Immunoscintigraphy of adenocarcinomas by means of radiolabeled F(ab')<sub>2</sub> fragments of an anti-carcinoembryonic antigen monoclonal antibody: a multicenter study. *Cancer Res* 1989;49:3095-3103.
23. Goldenberg DM, Goldenberg H, Sharkey RM, et al. Clinical studies of cancer radioimmunodetection with carcinoembryonic antigen monoclonal antibody fragments labeled with <sup>123</sup>I or <sup>99m</sup>Tc. *Cancer Res* 1990;50:909s-921s.
24. Epenetos AA, Britton KE, Mather S, et al. Targeting of Iodine-123 labeled tumor-associated antibodies to ovarian, breast and gastrointestinal tumours. *Lancet* 1982;2:999-1005.
25. Abdel-Nabi HH, Schwartz AN, Goldfogel G, et al. Colorectal tumors: scintigraphy with In-111 anti-CEA monoclonal antibody and correlation with surgical, histopathologic, and immunohistochemical findings. *Radiology* 1988;166:747-752.
26. Baum RP, Hertel A, Lorenz M, Schwarz A, Encke A, Hor G. <sup>99m</sup>Tc-labeled anti-CEA monoclonal antibody for tumour immunoscintigraphy: first clinical results. *Nucl Med Commun* 1989;10:345-352.
27. Goldenberg DM, Goldenberg H, Ford EH, et al. Initial clinical imaging results with a new Tc-99m-antibody labeling method [Abstract]. *J Nucl Med* 1989;30:809.
28. Berche C, Mach JP, Lumbroso JD, et al. Tomoscintigraphy for detecting gastrointestinal and medullary thyroid cancers: first clinical results using radiolabelled monoclonal antibodies against carcinoembryonic antigen. *Br Med J* 1982;285:1447-1451.
29. Baum RP, Lorenz M, Hor G. Radioimmunsintigraphie bei kolorektalen Karzinomen—Stellenwert in der Rezidivdiagnostik nach 2 Jahren klinischer Erfahrung. *Nuklearmedizin* 1987;10:219-234.
30. Kramer EL, Sanger JJ, Walsh C, et al. Contribution of SPECT to imaging of gastrointestinal adenocarcinoma with <sup>111</sup>In-labeled anti-CEA monoclonal antibody. *AJR* 1988;151:697-703.
31. Delaloye B, Bischof-Delaloye A, Buchegger F, et al. Detection of colorectal carcinoma by emission-computerized tomography after injection of <sup>123</sup>I-labeled Fab' or F(ab')<sub>2</sub> fragments from monoclonal anti-carcinoembryonic antigen antibodies. *J Clin Invest* 1986;77:301-311.
32. Bischof-Delaloye A, Delaloye B, Buchegger F, et al. Clinical value of immunoscintigraphy in colorectal carcinoma patients: a prospective study. *J Nucl Med* 1989;30:1646-1656.
33. Primus FJ, Freeman JW, Goldenberg DM. Immunological heterogeneity of carcinoembryonic antigen: purification from meconium of an antigen related to carcinoembryonic antigen. *Cancer Res* 1983;43:679-685.
34. Primus FJ, Newell KD, Blue A, Goldenberg DM. Immunological heterogeneity of carcinoembryonic antigen: antigenic determinants on carcinoembryonic antigen distinguished by monoclonal antibodies. *Cancer Res* 1983;43:686-692.
35. Primus FJ, Kuhns WJ, Goldenberg DM. Immunological heterogeneity of carcinoembryonic antigen: immunohistochemical detection of carcinoembryonic antigen determinants in colonic tumors with monoclonal antibodies. *Cancer Res* 1983;43:693-701.
36. Hansen HJ, Newman ES, Ostella F, Moskie LA, Sharkey RM, Goldenberg DM. Preclinical comparison of two specific anti-carcinoembryonic antigen (CEA) MAbs, NP-4 and IMM-14, in athymic nude mice bearing GW-39 colon carcinoma xenografts [Abstract]. *Cancer Res* 1989;30:414.
37. Greenwood FC, Hunter WM, Glover JS. The preparation of <sup>131</sup>I-labeled human growth hormone of high specific radioactivity. *Biochem J* 1963;89:114-123.
38. Sharkey RM, Primus FJ, and Goldenberg DM. Antibody protein dose and radioimmunodetection of GW-39 human colon tumor xenografts. *Int J Cancer* 1987;39:611-617.
39. ImmuSTRIP-HAMA IgG, Package Insert, April 1988.

40. ImmuSTRIP-HAMA IgG, Package Insert, July 1990.
41. Keenan AM, Harbert JC, Larson SM. Monoclonal antibodies in nuclear medicine. *J Nucl Med* 1985;26:531-537.
42. Larson SM. Lymphoma, melanoma and colon cancer: diagnosis and treatment with radiolabeled monoclonal antibodies. The 1986 Eugene Pendergrass New Horizons Lecture. *Radiology* 1987;165:297-304.
43. Goldenberg DM. Current status of cancer imaging with radiolabeled antibodies. *J Cancer Res Clin Oncol* 1987;113:203-208.
44. Goldenberg DM. Targeting of cancer with radiolabeled antibodies: prospects for imaging and therapy. *Arch Pathol Lab Med* 1988;112:580-587.
45. Schlom J. Innovations in monoclonal antibody tumor targeting: diagnostic and therapeutic implications. *JAMA* 1989;261:744-746.
46. Larson SM. Clinical radioimmunodetection, 1978-1988: overview and suggestions for standardization of clinical trials. *Cancer Res* 1990;50:892s-898s.
47. Maguire RT, Schmelter RF, Pasucci VL, Conklin JJ. Immunoscintigraphy of colorectal adenocarcinoma; results with site-specifically radiolabeled B72.3 (<sup>111</sup>In-Cyt-103). *Antib Immunoconjug Radiopharm* 1989;2:257-269.
48. Maguire R, Pascucci V, Maroli A, Schmelter R, Conklin J, McKearn T. Immunoscintigraphy of colorectal cancer: multicenter clinical trials with <sup>111</sup>In-Cyt-103 (OncoScint 103). *Antib Immunoconjug Radiopharm* 1990;3:39.
49. Day ED. Vascular relationships of tumor and host. *Progr Exp Tumor Res* 1964;4:57-97.
50. Jain RK. Determinants of tumor blood flow: a review. *Cancer Res* 1988;48:2641-2658.
51. Larson HJ, Jones AL, Sharkey RM, et al. Preclinical evaluation of an "instant" <sup>99m</sup>Tc-labeling kit for antibody imaging. *Cancer Res* 1990;50:794s-798s.

(continued from page 23)

## **SELF-STUDY TEST**

# **Pulmonary Nuclear Medicine**

### **ANSWERS**

#### **ITEMS 1-3: Unilateral Pulmonary Hypoventilation and Hypoperfusion**

ANSWERS: 1, F; 2, F; 3, F

Central pulmonary airway hyperdeposition of radioaerosols is frequently associated with poor peripheral penetration of activity. In fact, prior to the development of convenient methods to produce submicronic radioaerosol droplets, central "hot spots" secondary to impaction of large particles commonly led to poor delineation of peripheral air spaces. The anterior and posterior radioaerosol images shown in Figure 1 reveal a substantial amount of radioaerosol activity at and just above the carina. This activity extends laterally into the region of the left central bronchi. However, there is excellent uniform peripheral penetration of radioaerosol activity in the left lung. Only the right lung shows markedly diminished aerosol activity, with a patchy distribution. Radioaerosol activity, however, does reach the lung periphery in several areas. There is no central right-sided aerosol hyperdeposition, nor are "hot spots" seen in more peripheral zones of the right lung. The lack of right-sided central airway hyperdeposition and the excellent penetration of activity to the outer zones of the left lung and the peripheral location of whatever activity has reached the right lung suggest that the aerosol particles were small enough to reach the lung periphery. The findings suggest that intrinsic pulmonary disease, present to a much greater extent in the right lung than the left, is responsible for the asymmetric deposition of activity, rather than central obstruction or central airflow turbulence. The central hyperdeposition in the trachea probably was caused by turbulent airflow, perhaps secondary to excessive mucus in the airways. The findings also demonstrate that centrally turbulent airflow will not prevent good penetration of submicronic radioaerosols to a well-ventilated lung in the absence of significant airway blockage.

Because inhalation and imaging of the <sup>99m</sup>Tc-labeled radioaerosol generally is performed before injection and imaging of the <sup>99m</sup>Tc MAA, the possibility always exists that <sup>99m</sup>Tc aerosol activity could contribute to and degrade the perfusion images. When both studies are properly performed, however, this is not a clinical problem. On the average, only about 700-800  $\mu$ Ci of radioaerosol is deposited in the lungs after a typical inhalation period of 2-3 minutes. A typical <sup>99m</sup>Tc MAA dose of approximately 4 mCi yields a perfusion image to aerosol image count-rate ratio of about 5:1. Under these circumstances, only areas of focal aerosol hyperdeposition are likely to be seen on the "combined" aerosol-perfusion image, and even these areas usually are not prominent. In Figure 1, note that the count rate for the aerosol images alone was 100,000 counts per 150 sec (about 660 counts/sec). After <sup>99m</sup>Tc MAA injection, the count rate was 400,000 counts per 60 sec (about 6660 counts/sec). Hence, the net count rate from <sup>99m</sup>Tc MAA was 6000 counts/sec. In this patient, the count rate contributed by <sup>99m</sup>Tc MAA was nearly ten times the aerosol count rate, making significant "shine-through" of the aerosol activity most unlikely. It has been shown that such "shine-through" is not a problem even when the <sup>99m</sup>Tc MAA to <sup>99m</sup>Tc DTPA count-rate ratios are as low as 4:1 or 5:1. In this example, the left central

airway activity still can be seen faintly on the perfusion images, as can tracheal activity and swallowed activity in the gastric fundus. The medial right lower lobe radioaerosol activity is not as intense as these foci on the original aerosol images. Accordingly, it is unlikely to be visible on the perfusion images. Thus, medial right lower lobe activity on the perfusion images more likely represents a region of maintained perfusion than an artifact caused by <sup>99m</sup>Tc aerosol activity.

The irregular and incomplete reduction of perfusion seen in this patient's right lung is not at all typical of postradiation change. In irradiated patients, perfusion is reduced in uniform fashion throughout the irradiated region, which usually has a well-defined geometric shape. At the radiation doses usually employed for bronchogenic carcinoma ( $\geq 5000$  rads midplane cumulative dose), perfusion is markedly reduced due to radiation-induced microvascular obliteration. Ventilation also may be reduced in the irradiated area, but usually it is much less affected than perfusion. When abnormal, ventilation studies typically reveal effects of reduced lung volume, and show a more uniform pattern of hypoventilation than seen in this image.

In this patient, Swyer-James' syndrome (unilateral hyperlucent lung) had been diagnosed many years previously. The origin of her disease was not known precisely, although she did report several episodes of bronchitis in childhood. Her chest radiograph revealed a moderately hyperlucent right lung and a normal-appearing left lung. The hypoventilation of her right lung was considered to be secondary to diffuse small airways obstructive disease on the right.

#### **ITEMS 4-8: Sarcoidosis**

ANSWERS: 4, F; 5, F; 6, T; 7, F; 8, F

Sarcoidosis is a systemic disorder characterized by enhanced local immune processes, which cause the most significant morbidity through their effects on the pulmonary parenchyma. Although the etiology of sarcoidosis is still unknown, and no direct relationship to an infectious agent has been shown, there appears to be a temporal association between the presence of an initial alveolitis and the subsequent development of granulomas and fibrosis. In most patients disease is self-limited and is associated with a good prognosis. Patients who present with symptoms of dyspnea are those who have more advanced disease, the greatest extent of pulmonary fibrosis, and who show the poorest response to therapy. Prognosis is partially determined by the appearance of the disease on chest roentgenograms. Nonetheless, many patients with persistently abnormal roentgenograms show no clinical evidence of progressive disease.

Although granulomas are the characteristic pathologic feature of the disease, the initial lesion in the lung is probably an alveolitis from which the granulomas eventually are derived. As a granuloma matures, there is an increase in the number of fibroblasts, which may lead to roentgenographically evident parenchymal fibrosis. The sarcoid granuloma either resolves, leaving no morphologic changes, or it undergoes an obliterative

(continued on page 74)